The Plant Defense Elicitor Cryptogein Stimulates Clathrin-Mediated Endocytosis Correlated with Reactive Oxygen Species Production in Bright Yellow-2 Tobacco Cells[1][C]

Nathalie Leborgne-Castel*, Jeannine Lherminier, Christophe Der, Jérôme Fromentin, Valérie Houot, and Françoise Simon-Plas

UMR INRA 1088/CNRS 5184/Université de Bourgogne, Plante-Microbe-Environnement, F–21000 Dijon, France

The plant defense elicitor cryptogein triggers well-known biochemical events of early signal transduction at the plasma membrane of tobacco (*Nicotiana tabacum*) cells, but microscopic observations of cell responses related to these early events were lacking. We determined that internalization of the lipophilic dye FM4-64, which is a marker of endocytosis, is stimulated a few minutes after addition of cryptogein to tobacco Bright Yellow-2 (BY-2) cells. This stimulation is specific to the signal transduction pathway elicited by cryptogein because a lipid transfer protein, which binds to the same receptor as cryptogein but without triggering signaling, does not increase endocytosis. To define the nature of the stimulated endocytosis, we quantified clathrin-coated pits (CCPs) forming on the plasma membrane of BY-2 cells. A transitory stimulation of this morphological event by cryptogein occurs within the first 15 min. In the presence of cryptogein, increases in both FM4-64 internalization and clathrin-mediated endocytosis are specifically blocked upon treatment with 5 μM tyrphostin A23, a receptor-mediated endocytosis inhibitor. The kinetics of the transient increase in CCPs at the plasma membrane coincides with that of transitory reactive oxygen species (ROS) production occurring within the first 15 min after elicitation. Moreover, in BY-2 cells expressing *NtrbohD* antisense cDNA, which are unable to produce ROS when treated with cryptogein, the CCP stimulation is inhibited. These results indicate that the very early endocytic process induced by cryptogein in tobacco is due, at least partly, to clathrin-mediated endocytosis and is dependent on ROS production by the NADPH oxidase NtrbohD.

The plasma membrane forms a barrier between the cell and the extracellular medium. Numerous functions are ascribed to this membrane, particularly environmental signal recognition and transduction of these signals into intracellular responses. Endocytosis is a process whereby portions of the plasma membrane invaginate and bud off to form membrane-bounded vesicles containing extracellular materials, as well as lipids and proteins incorporated on the cell surface (Pastan and Willingham, 1985). Animal cells use multiple endocytotic tracks to respond to the external environment. Some concern the fluid-phase uptake either by phagocytosis, whereby cells may simply internalize particles or organisms, like bacteria, or by macro pinocytosis, whereby cells internalize soluble materials. Others are related to membrane microdomains enriched in cholesterol and glycerosphingolipids, including lipid rafts and caveolae (Parton and Richards, 2003). The latter contain integral proteins, named caveolins, specific to particular cell types and having a central role in the formation of caveolae involved in endocytosis.

The best-studied type of endocytosis is clathrin-associated endocytosis. In animal cells, a high-profile function for endocytosis is the receptor-mediated uptake (receptor-mediated endocytosis [RME]) that uses clathrin-coated pits (CCPs) as vehicles for receptor/cargo internalization by forming clathrin-coated vesicles (CCVs) after vesicle scission. Clathrin is the accepted central structural scaffold of receptor-internalizing endocytotic pits and the main endocytic route in many animal cells (Brodsky, 1988). The coat of CCVs is a polygonal lattice, which contains two main components surrounding the vesicle membrane: clathrin and adaptor protein (AP) complexes. Coated-pit assembly is thought to be initiated by the binding of the AP-2 μ2 subunit of the adaptor complex to a specific cytosolic domain, corresponding to an endocytotic signal, of a receptor/transmembrane protein (Bonifacino and Traub, 2003). Some RME inhibitors, such as specific tyrphostins, interact in vitro with these endocytotic signals and thus prevent interaction of these domains with μ2 chain subunits of the clathrin-associated adaptor complex

[1] This work was supported by grants from the MNERT, the Conseil Régional de Bourgogne, and the Agence Nationale de la Recherche (grant no. JC05–50610).

* Corresponding author; e-mail nathalie.leborgne-castel@dijon.inra.fr.

The author responsible for distribution of materials integral to the findings presented in this article in accordance with the policy described in the Instructions for Authors (www.plantphysiol.org) is: Nathalie Leborgne-Castel (nathalie.leborgne-castel@dijon.inra.fr).

[C] Some figures in this article are displayed in color online but in black and white in the print edition.

www.plantphysiol.org/cgi/doi/10.1104/pp.107.111716

(Crump et al., 1998). Tyrphostin A23 has been specifically used in mammalian cells to inhibit internalization of a receptor internalized via CCVs: the transferrin receptor (Tf-R; Banbury et al., 2003).

When specific ligands involved in processes such as signal transduction and nutrient transport bind to their plasma membrane receptors, the resulting complexes are commonly internalized by endocytosis. The influence of ligand binding on receptor endocytosis distinguishes two types of internalization. In constitutive clathrin endocytosis, all receptors are internalized, whether they are bound to their ligand or not. Receptors endocytosed in this way include receptors mediating the uptake of nutrients (e.g. Tf-R; Watts, 1985). In contrast, receptors are internalized during ligand-induced endocytosis only upon activation resulting from the binding of their specific ligand (e.g. epidermal growth factor receptor [EGFR]; Beguinot et al., 1984).

Although the study of cell surface receptors undergoing endocytosis has recently been extended, the role of this process in cell signaling is far from being fully understood. This process is thought to desensitize cell responses by internalizing the receptor, but it also moves the receptor away from the plasma membrane to elicit downstream signaling (González-Gaitán, 2003).

Evidence for RME in plants was provided by Horn et al. (1989), using saturable and temperature-dependent uptake of labeled plant defense elicitors into cells. However, plasma membrane receptor-ligand interactions are frequently incompletely characterized. The involvement of endocytotic processes of receptors for signal transduction during plant development has been discovered only recently (Shah et al., 2002; Russinova et al., 2004; Gifford et al., 2005; Kwaaitaal et al., 2005). Shah et al. (2002) suggested that only cells showing endocytosis of the receptors are actively engaged in ligand-mediated signaling. In a plant defense context, mutation of the C-terminal domain of an ethylene-inducing xylanase receptor, containing a well-known mammalian endocytotic signal, abolished its ability to induce the hypersensitive response (HR), suggesting that endocytosis plays a key role in the corresponding signal transduction pathway (Ron and Avni, 2004). Two types of receptor uptake have been described very recently in plant cells: evidence for specific ligand-induced uptake of the bacterial elicitor flagellin Leu-rich repeat (LRR) receptor was reported by Robatzek et al. (2006), and ligand-independent trafficking has been shown for the steroid BRI1 LRR receptor (Geldner et al., 2007). Moreover, this latter study argues that the endosomal pool of BRI1 is functional so that signal transduction takes place after endocytosis, suggesting that endosomes act as signaling compartments in plant cells (Geldner et al., 2007).

The nature of endocytosis in plant cells is still a matter of debate. Morphological similarities with animal cells (e.g. CCPs and CCVs), and the existence of plant homologs of proteins involved in clathrin-mediated endocytosis, suggest that this pathway takes place in plant cells (Low and Chandra, 1994; Holstein, 2002; Murphy et al., 2005). Moreover, clathrin-dependent endocytosis has been shown very recently to be operational in plants and used as a predominant pathway, as in animal cells, for internalization of plasma membrane proteins, such as the auxin carrier PIN1 in Arabidopsis (*Arabidopsis thaliana*), and for spindle and phragmoplast formation as well as for endocytosis in tobacco (*Nicotiana tabacum*) Bright Yellow-2 (BY-2) cells (Dhonukshe et al., 2007; Tahara et al., 2007). In addition, endocytosis of the human Tf-R, known to be clathrin-dependent in animal cells, is inhibited by an RME inhibitor after expression in plant protoplasts, suggesting the existence of clathrin machinery for RME in plant cells (Ortiz-Zapater et al., 2006). Nevertheless, even if recent evidence for the involvement of vesicle trafficking in the plant immune response against pathogens has been reported (Robatzek, 2007), data are lacking concerning the nature of endocytosis in a plant defense context.

A number of specific molecules elicit defense responses in plant cells during plant pathogen interactions. Cryptogein, produced by the oomycete *Phytophthora cryptogea*, belongs to a class of proteinaceous elicitors called elicitins, able to induce a HR and acquired resistance in tobacco plants (Ricci et al., 1989). The mode of action of cryptogein begins with the recognition of this elicitor by an unidentified plasma membrane receptor at a high-affinity binding site (Wendehenne et al., 1995). This ligand-receptor binding triggers a cascade of events that include phosphorylation processes, rapid calcium influx, ion effluxes, nitric oxide production, extracellular alkalinization, and plasma membrane depolarization both in tobacco plants and cell suspensions (Blein et al., 1991; Tavernier et al., 1995; Wendehenne et al., 2002; Garcia-Brugger et al., 2006). In addition, the activation of a membrane-bound NADPH oxidase (NtrbohD), responsible for reactive oxygen species (ROS) production, has been shown in cryptogein-elicited cells (Simon-Plas et al., 1997, 2002). These rapid biochemical alterations at the plasma membrane subsequent to cryptogein treatment are well described, but there has been no study of associated structural modifications at the plasma membrane level. In this article, we report that cryptogein stimulates overall endocytosis in BY-2 tobacco cells. Using transmission electron microscopy (TEM) and pharmacological interference, we provide evidence that ligand-stimulated endocytosis concerns the clathrin-dependent pathway. Moreover, we suggest that transitory ROS production triggered by cryptogein elicitation takes part in the stimulation of clathrin-mediated endocytosis.

RESULTS

Cryptogein Induces Modifications of Spectral Properties and Internalization of FM4-64 at the Plasma Membrane

To assess the intervention of endocytosis in the signaling pathway triggered by cryptogein, we analyzed the time course of internalization of the endocytotic

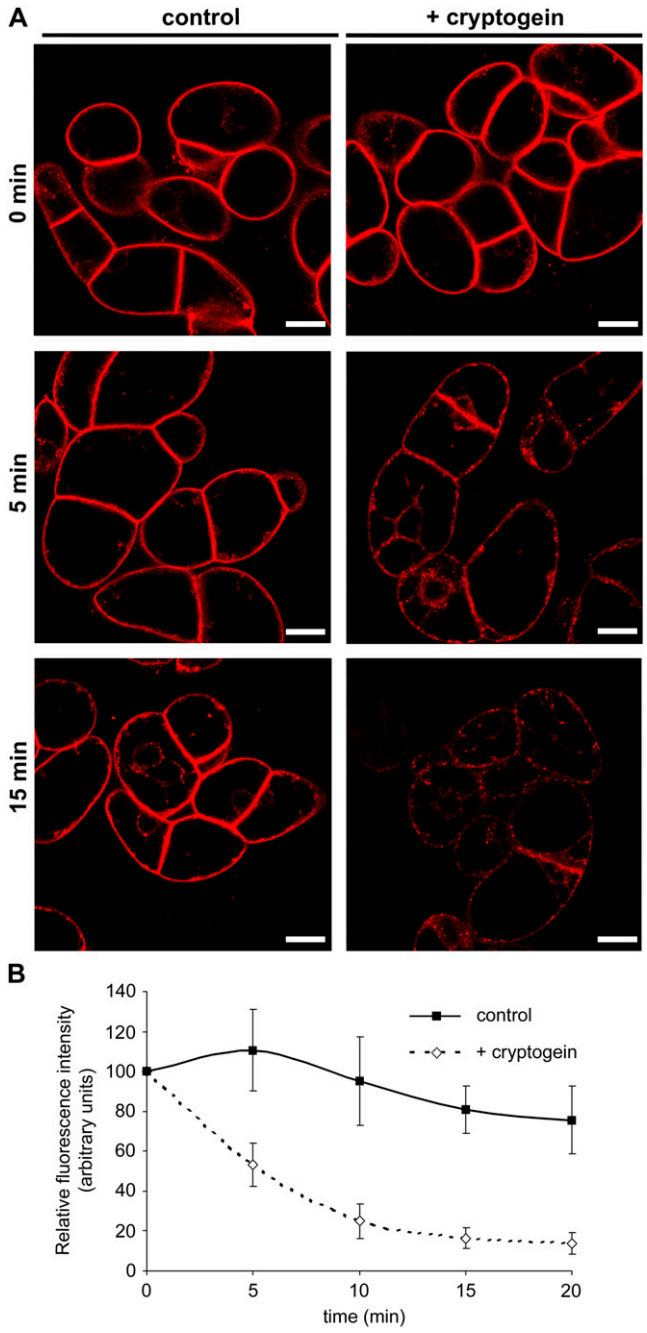

Figure 1. Cryptogein modifies spectral properties of FM4-64 on plasma membrane. A, Confocal sections of 7-d-old BY-2 tobacco cells labeled with FM4-64 (4.25 μM) for 5 min (top; 0 min), then incubated in the presence or absence of cryptogein for 5 min (middle; 5 min) or 15 min (bottom; 15 min) under constant agitation at 23°C in the dark. Left, Control cells; right, cells plus 50 nM cryptogein. All image acquisition parameters were kept constant for imaging control and cryptogein-treated cells. Bars = 20 μm. B, Measurements of FM4-64 fluorescence at the plasma membrane level using the Image J software. Data are mean values and SD from eight independent experiments.

marker FM4-64 in BY-2 cells using confocal laser microscopy (Betz et al., 1996; Bolte et al., 2004). After 5-min exposure, FM4-64 strongly labeled the plasma membrane as a result of dye partitioning into the lipid phase (Fig. 1A; 0 min [top]).

Following cryptogein treatment, we could observe a drastic time-dependent drop in FM4-64 fluorescence at the plasma membrane (Fig. 1A). Fluorescence quantification indicated an 80% to 90% decline in dye fluorescence at the plasma membrane immediately after cryptogein treatment (Fig. 1B). Given that FM dyes originate from dimethylaminostyrylmethyl-pyridinium iodine, used as an electric potential-sensitive probe in studies of mitochondria (Betz et al., 1992), FM4-64 may respond to transmembrane potential modifications. Indeed, fluorescence of styryl dyes has been described as voltage dependent and sensitive to ion/proton concentration. The decrease in plasma membrane fluorescence correlates with previous electrophysiological measurements of plasma membrane depolarization in elicited cells (Pugin et al., 1997). Dye fluorescence slightly increased in untreated cells, which may correspond to continuous loading of FM4-64 at the plasma membrane, and then decreased gradually (Fig. 1B). The observed 10% decrease in fluorescence could be explained by light stress bleaching the dye during sampling or its instability at room temperature (Bolte et al., 2004). It should be noted that emerging cell plates of dividing cells, previously described for their intense FM4-64 fluorescence (Bolte et al., 2004; Dhonukshe et al., 2006), were not affected by elicitor treatment (Fig. 1A, right).

In spite of the decrease in plasma membrane fluorescence in elicited cells, fluorescent endocytotic membrane-bound or internalized vesicles could still be observed within cells (Figs. 1A and 2B). Endocytotic vesicle emergence was monitored in cryptogein-treated cells in comparison to controls. Figures 1A and 2B show that 5 min of cryptogein treatment (corresponding to 10-min FM4-64 loading) were sufficient to activate marked internalization of the fluorescent dye, whereas untreated cells presented intense plasma membrane staining and only a few internalized vesicles. Both treated and untreated cells underwent endocytosis after 15 min, but the number of fluorescent vesicles differed between cells: Numerous membrane-bound and internalized vesicles were visible in cryptogein-treated cells, whereas untreated cells showed a significantly lower amount of fluorescent vesicles (Fig. 1A, bottom).

A decrease of fluorescence of the inner vesicles was also observed after 10 min of cryptogein treatment (Fig. 2A), but it is very low compared to the marked decrease of the whole plasma membrane fluorescence. This suggests that vesicles present inside the cells at that time were preformed before alteration of plasma membrane properties induced by the elicitor leading to fluorescence decrease.

To perform global statistical analysis, fluorescent vesicles appearing in control and elicited cells were quantified in eight independent experiments (Fig. 2B). Optical sections of cells were classified into three groups, corresponding to cells with only plasma membrane labeling (0) and cells containing few (1–10)

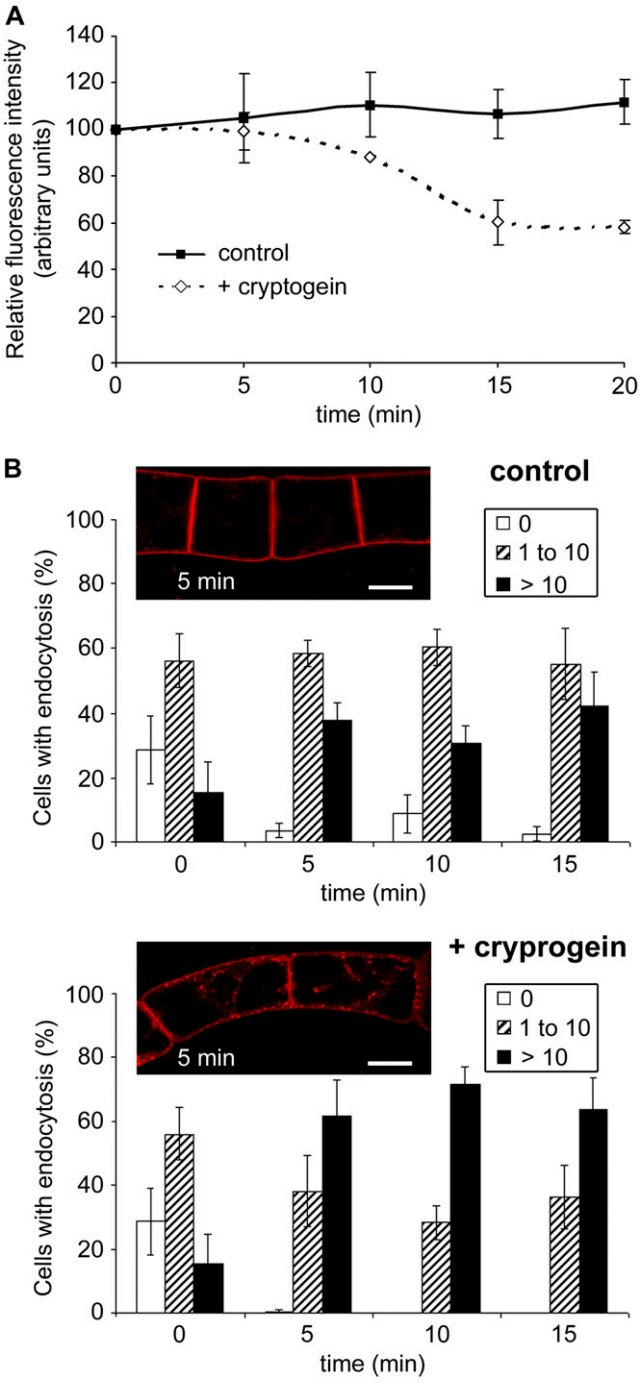

Figure 2. Increasing FM4-64 internalization within BY-2 cells in the presence of cryptogein. Seven-day-old tobacco BY-2 cells were labeled with FM4-64 (4.25 μM) for 5 min (time 0 min) at 23°C or treated in the presence or absence of cryptogein (50 nM). Cells were kept under constant agitation in the dark. A, Measurements of FM4-64 fluorescence of vesicles in control cells (continuous line), or subsequent to cryptogein treatment (dashed line). Data are mean values and SD from four independent experiments. B, Quantification of control and cryptogein-treated cells showing endocytosis during time. Data are presented as percentage of cells (*n* approximately 30–50) corresponding to class 0, no endocytosis (white columns); class 1 to 10, 1 to 10 vesicles (dashed columns); class >10, more than 10 vesicles (black columns). Data are mean values and SD from eight independent experiments. Inset, Images of BY-2 untreated (control) or cryptogein-treated cells after 5 min (corresponding to 10 min FM4-64 loading) are presented. Bars = 20 μm. [See online article for color version of this figure.]

visible vesicles or more than 10 vesicles (>10). The percentage of cells belonging to the three groups was measured over time. The percentage of cells with endocytosis increased concomitantly with a decrease in cells without fluorescent vesicles both for elicited and untreated cells. However, the number of fluorescent vesicles appearing in elicited cells was higher, even if counting of fluorescent vesicles was underestimated due to the decrease in fluorescence in these cells. Indeed, 100% of cells contained fluorescent vesicles after 10 min of elicitation, with 70% containing more than 10 vesicles, whereas at this same time point untreated cells still presented 10% of cells without endocytosis and only 30% contained more than 10 vesicles (Fig. 2B).

These results indicate that FM4-64 uptake into BY-2 cells is rapidly stimulated by cryptogein, suggesting the occurrence of an endocytotic process triggered by the elicitor. Moreover, these results support the idea that FM4-64 dye may be used not only for studying endocytosis, but also for tracking modification of membrane properties.

Endocytosis Requires Not Only Binding to the Receptor, But Also Downstream Signaling Events

To examine whether endocytosis is triggered by ligand-receptor binding and/or by subsequent signaling events, we used a lipid transfer protein (LTP) previously demonstrated to share some structural and plasma membrane-binding properties with elicitins (Blein et al., 2002). In tobacco cells, both cryptogein and an LTP1 from wheat (*Triticum aestivum*) bind to an identical high-affinity specific site located on the plasma membrane (Buhot et al., 2001). In addition, in vivo competition experiments have indicated that the binding sites for both proteins are their true biological receptor because addition of increasing concentrations of LTP1 reduced signaling events induced by cryptogein (Buhot et al., 2001). Nevertheless, LTP alone did not trigger any of the classical responses induced by cryptogein in tobacco cells, such as extracellular alkalinization or oxidative burst.

The effect of 500 nM LTP (which represents a 10-fold higher concentration than that of cryptogein) on BY-2 cell endocytosis was analyzed using the FM4-64 dye. Figure 3 shows cells undergoing full endocytosis (>10 fluorescent vesicles per confocal section of cells) in control, cryptogein-treated, and LTP-treated cells. In LTP-treated cells, the observed endocytosis resembled that in control cells, whereas endocytosis was stimulated in cryptogein-treated cells. Moreover, FM4-64 dye fluorescence in LTP-treated cells, indicative of the modification of plasma membrane properties, was not affected (data not shown).

These results indicate that the binding of LTP to its cryptogein-shared receptor is not sufficient to induce either endocytosis or signaling responses. Consequently, the endocytosis phenomenon can be correlated with signaling events specifically triggered by cryptogein.

Cryptogein Induces an Increase in CCP Density

To further scrutinize endocytosis, plasma membrane ultrastructure was examined in control and cryptogein-treated cells (Fig. 4). Pits with an electron-dense coating were clearly visible at the plasma membrane surface. They appeared as flat, curved, or invaginated coated regions of 100, 75, and 50 nm, respectively (Fig. 4, A–C, arrows). These pits resembled CCPs, already described in plant cells (Low and Chandra, 1994; Robinson et al., 1998) and recently confirmed to be so using antipeptide antibodies directed against plant clathrin (Dhonukshe et al., 2007). In some cells, CCVs (Fig. 4D, arrowheads) or multivesicular bodies (MVBs; Fig. 4E) were also observed within the cytosol.

The CCPs were quantified per approximately 100 μm of plasma membrane in sections of untreated and cryptogein-treated cells. The different stages of pinching off of CCPs before scission (Fig. 4, A–C) were taken into account for quantification. Each cell section was classified into three groups: without CCP (0 CCP; class 0), with one CCP (class 1), and with two or more CCPs (class 2). Data are presented as percentages of cells belonging to these groups after different times of cryptogein treatment (Fig. 4F). When sections of untreated cells (control) were observed, most of them did not present any CCP, 24% belonged to class 1, and only 3% contained two or more CCPs (class 2) on their plasma membrane surface (Fig. 4F). On the contrary, after 10 min of cryptogein treatment, >90% of cell sections presented CCPs (classes 1 and 2) of which 12% had two or more CCPs (Fig. 4F). After 20 min of cryptogein treatment, the number of CCPs decreased concomitantly with an increase in CCVs (Fig. 4D, arrowheads) and MVBs (Fig. 4E). At this time point, even if the percentage of cell sections showing endocytosis was high (62%), only 1% of them presented two or more CCPs (Fig. 4, F and G). This can be interpreted as a reduction of the de novo clathrin-coated endocytosis induced by cryptogein. After 45 min, the percentage of elicited cells presenting CCPs resembled that of the control (data not shown).

To summarize all the results and to present the entire kinetics of CCP up to 20 min, we calculated the ratio of all CCP groups relative to the control (beginning of the experiment) in both untreated and cryptogein-treated cells (Fig. 4G). In treated cells, a rapid transitory rise was observed in CCPs 5 to 10 min after cryptogein addition, and then a constant decrease. On the contrary, untreated cells presented a more or less constant percentage of the three classes of CCP, corresponding to a steady-state number of CCPs on the plasma membrane of the cells.

These indicate that cryptogein triggers massive transitory formation of CCPs at the plasma membrane and, consequently, clathrin endocytosis from the plasma membrane in BY-2 cells. This sudden wave of endocytosis after cryptogein elicitation, taken together with FM4-64 internalization measurements, confirms that endocytosis is an early event of this signaling pathway.

Cryptogein-Stimulated Endocytosis Is Blocked by Tyrphostin A23

Following the TEM results showing a transitory increase in CCP number after cryptogein treatment, we applied a RME inhibitor belonging to the tyrphostin family to cells. Tyrphostins are chemical compounds structurally analogous to the side chain of Tyr that were originally developed as substrate-competitive inhibitors of the EGFR Tyr kinase (Gazit et al., 1989). Some tyrphostin members such as tyrphostin A23 have also been used to inhibit endocytosis: specific inhibition of clathrin-mediated endocytosis due to the interaction between tyrphostin A23 and the subunit μ2 of the AP-2 complex, one component of the membrane coat associated with clathrin, has been reported (Banbury et al., 2003). This inhibitor has been used at concentrations of 500 or 350 μM in mammalian cells to inhibit internalization of the Tf-R (Banbury et al., 2003) or the prion protein (Taylor et al., 2005), and in plant protoplasts to inhibit human Tf-R internalization (Ortiz-Zapater et al., 2006). More recently, tyrphostin A23 was utilized at a concentration of 30 μM to inhibit internalization of the PIN auxin efflux carrier and different plasma membrane proteins in Arabidopsis roots (Dhonukshe et al., 2007). In these studies, tyrphostins inactive for RME inhibition (e.g. tyrphostin A51) were used to confirm the specific effect of tyrphostin A23.

Because of the Tyr kinase inhibitory effect of tyrphostins, which could disturb cryptogein signaling, we used a lower concentration compared to previous studies. The effect of 5 μM of the two tyrphostins was

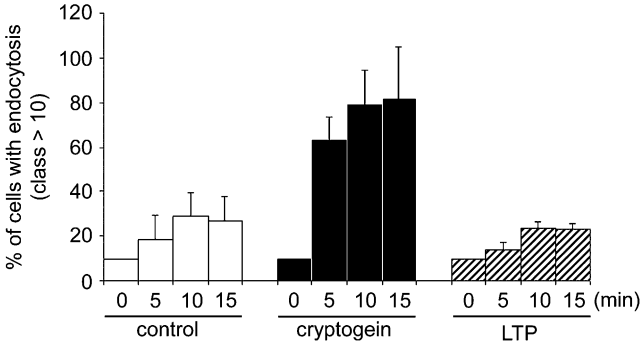

Figure 3. LTP1 from wheat does not modulate endocytosis. Effect of 500 nM LTP from wheat (LTP1; dashed columns) on the percentage of cells containing more than 10 vesicles. The kinetics of FM4-64 internalization in cells exposed to LTP is comparable to control cells (white columns), whereas cryptogein-treated cells show stimulated endocytosis (black columns). Mean and SD values are from three independent experiments.

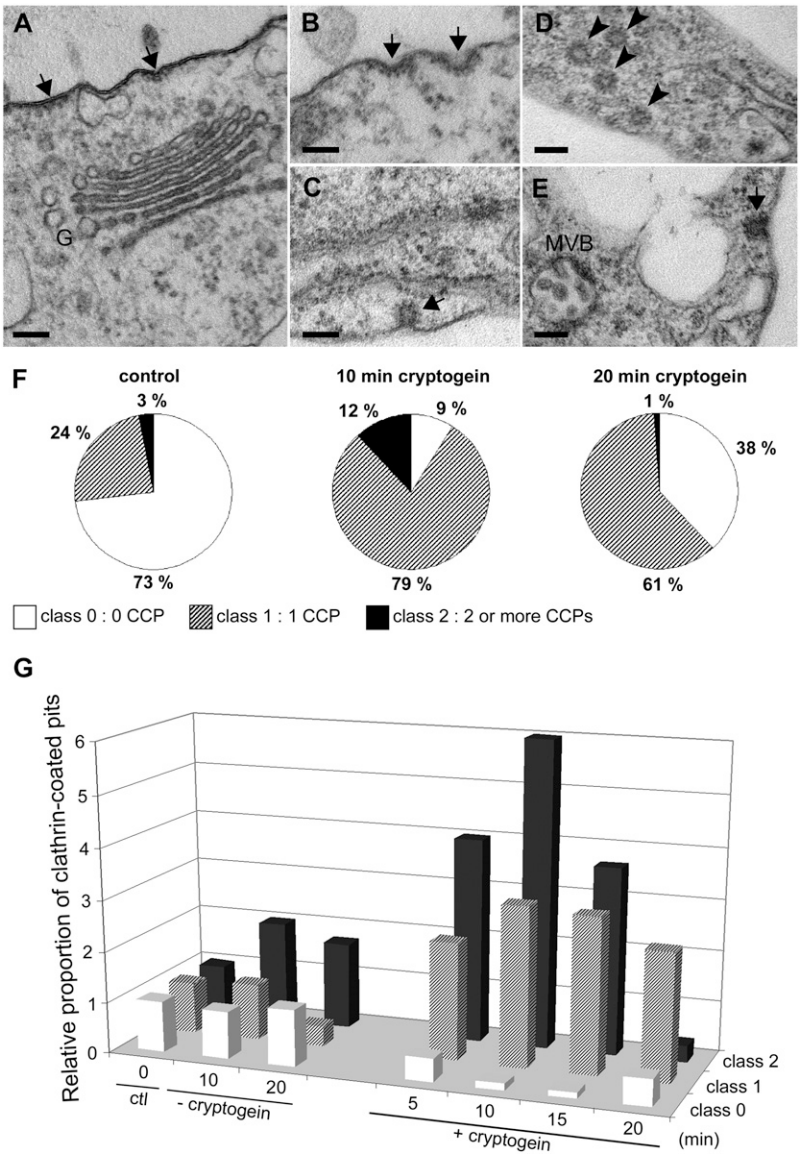

Figure 4. Cryptogein stimulates CCP formation at the plasma membrane. Plasma membrane of BY-2 cells was imaged by TEM. CCPs (arrows) were observed and quantified on 20 to 30 cell sections per 100-μm plasma membrane perimeter. A to E, Micrographs of different stages of CCP invagination before scission. Coated pits (arrows, A, B, C, E), coated vesicles (arrowheads, D). G, Golgi apparatus. Bars = 100 nm. F, Percentage of cell sections in the three classes of CCPs corresponding to no CCP (class 0; white portion), one CCP (class 1; dashed portion), or two or more CCPs (class 2; black portion) in control cells and at 10 and 20 min of cryptogein treatment. G, Relative increase of CCPs during the first 20 min in cells without or with 50 nM cryptogein treatment compared to control cells (ctl, 0 min).

analyzed by TEM imaging and the CCPs quantified, as previously. Experiments were carried out in two independent experiments, where cells presented different stages of steady-state endocytosis. Results are presented as relative amounts of CCPs triggered by cryptogein, compared to controls in the presence of tyrphostin alone (Fig. 5, A and B). Formation of CCVs was no longer triggered by cryptogein in the presence of tyrphostin A23 (Fig. 5A). However, tyrphostin A51-treated cells still exhibited cryptogein-stimulated clathrin-related endocytosis, although a slight decrease could be observed (Fig. 5B).

In addition, the effect of tyrphostins on FM4-64 uptake in the presence of cryptogein was tested. The proportion of cells undergoing full endocytosis (>10 vesicles per observed section) was calculated in controls plus dimethyl sulfoxide (DMSO), cryptogein-treated plus DMSO, or tyrphostin(s) plus cryptogein-treated cells (Fig. 5C). Results indicated a differential effect of the two tyrphostins on FM4-64 internalization stimulated by cryptogein. Indeed, tyrphostin A51-treated cells in the presence of cryptogein behaved similarly to cryptogein-treated cells, indicating that cryptogein-stimulated endocytosis is not affected by this compound. In contrast, tyrphostin A23-treated cells in presence of cryptogein undergo the same level of endocytosis as control cells (DMSO treated), showing inhibition of the stimulated endocytosis (Fig. 5C). These compounds had no effect on constitutive endocytosis, whereas cells treated with tyrphostins alone presented the same level of endocytosis as controls (data not shown).

The question was next addressed whether pharmacological disturbance of RME has an effect on two events known to occur after cryptogein elicitation, namely, extracellular alkalinization and transient ROS production (Fig. 5, D and E). Figure 5D presents the

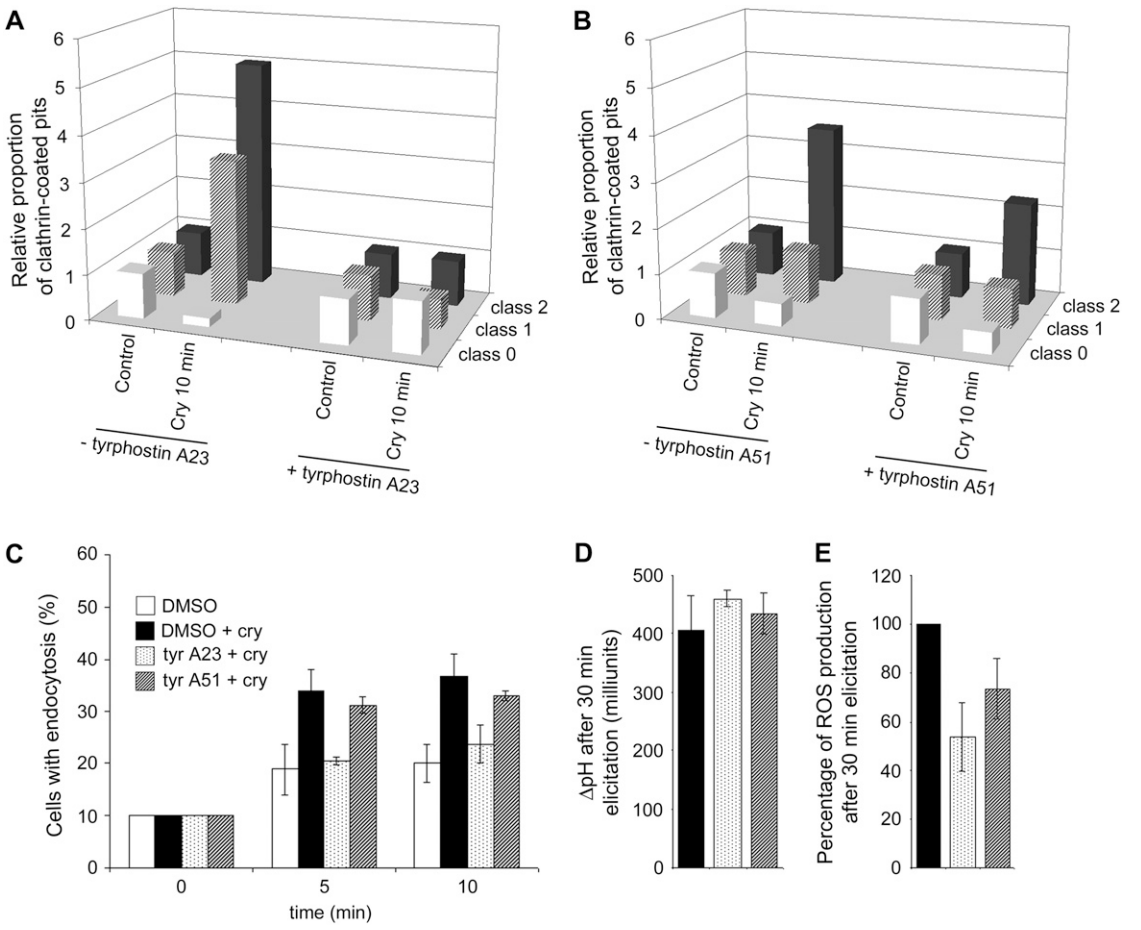

Figure 5. Tyrphostin A23, but not tyrphostin A51, prevents endocytosis in cryptogein-elicited BY-2 cells (A and B). Quantification of CCPs per 100-μm plasma membrane of 7-d-old BY-2 cells imaged by TEM. A, Relative increase of CCPs in elicited cells was compared in the presence and absence of tyrphostin A23. B, Relative increase of CCPs in elicited cells was compared in the presence and absence of tyrphostin A51. C, Seven-day-old BY-2 cells were labeled with FM4-64 (4.25 μM) for 5 min (0 min), then incubated with 0.1% DMSO (white columns), 0.01% DMSO plus 50 nM cryptogein (black columns), 5 μM tyrphostin A23 plus 50 nM cryptogein (spotted columns), or 5 μM tyrphostin A51 plus 50 nM cryptogein (dashed columns) under constant agitation at 23°C in the dark. BY-2 cells (*n* approximately 30–50) presenting full endocytosis (>10 vesicles) were quantified as described in Figure 2B. D, Extracellular ΔpH was measured in cells challenged with 50 nM cryptogein for 30 min in presence of 0.1% DMSO (control, black columns), 5 μM tyrphostin A23 (spotted columns), or 5 μM tyrphostin A51 (dashed columns). All treated cells exhibited extracellular alkalinization and no significant difference was observed. E, Effect of 5 μM tyrphostins on cryptogein-induced extracellular ROS production during the first 30 min after elicitor treatment. Total ROS production measured during 30 min of treatment by cryptogein was summed and expressed in percentage of ROS production in cells treated with cryptogein plus DMSO. Cells treated with cryptogein plus DMSO (black columns), cryptogein plus 5 μM tyrphostin A23 (spotted columns), or cryptogein plus 5 μM tyrphostin A51 (dashed columns).

extracellular ΔpH after 30 min of elicitation by cryptogein. In the presence of cryptogein plus DMSO, a standard increase of 400 milliunits of pH was observed. This increase remained constant regardless of which tyrphostin was added (Fig. 5D). Second, ROS production 30 min after elicitation by cryptogein is 40% reduced by tyrphostin A23 treatment and slightly less by tyrphostin A51 (Fig. 5E). These results indicate that both tyrphostins (active and inactive inhibitors of RME) affect ROS production when used at 5 μM, whereas the effect on endocytosis is different (Fig. 5).

The observations on FM4-64 uptake and CCP formation, together with use of pharmacological approaches, demonstrate that cryptogein-stimulated endocytosis is specifically inhibited by the RME inhibitor, tyrphostin A23, but not by its inactive analog tyrphostin A51. These results indicate that the elicitor-stimulated clathrin endocytosis, consecutive to receptor binding and signaling, may be due to an RME-mediated mechanism.

Cryptogein-Stimulated Clathrin Endocytosis Is Inhibited in Cells That Are Unable to Produce ROS

Not only binding of cryptogein to its putative receptor, but also the associated downstream signaling

events, are necessary for transitory increases in endocytosis, as shown using the LTP (Fig. 3). Moreover, the kinetics of transitory CCP increase corresponds to the kinetics of ROS production triggered by the elicitor (Simon-Plas et al., 1997). Thus, the next question to be addressed was whether ROS production could be correlated with endocytosis.

A BY-2 cell line (named gp3) was previously obtained expressing an antisense construction of *NtrbohD* cDNA, which is unable to produce ROS when treated with cryptogein, but still responds to the elicitor by an increase in extracellular pH (Simon-Plas et al., 2002) and membrane depolarization (this study; data not shown), similar to wild-type cells.

Gp3 cells were submitted to cryptogein and compared to untreated cells (Fig. 6). The quantification of CCPs in gp3 cell sections indicated that cryptogein did not stimulate de novo CCP formation (Fig. 6B).

Interestingly, the plasma membrane morphology of gp3 cells, submitted or not to cryptogein treatment, had principally flat pits delimited by a coat of dense particles (Fig. 6A, arrows). The detailed measurement of CCP diameters (reflecting their invagination) indicated that wild-type cells contained a low number of flat pits when compared to gp3 in spite of the same number of total pits, indicating a slowing down of CCP formation during constitutive endocytosis (Fig. 6C). Moreover, the percentage of flat pits in gp3 did not change after cryptogein elicitation, whereas it decreased concomitantly with an increase in curved to invaginated CCPs in wild-type cells (Fig. 6C). These results indicate that cryptogein-stimulated formation of CCVs is not triggered in gp3 cells. Interestingly, western-blot analysis using antisera directed against the human clathrin heavy chain revealed no difference in clathrin amounts in the plasma membrane between the two untreated cell lines, nor 5 or 15 min after cryptogein treatment (data not shown). These results suggest that the determining factor for formation of CCVs is not the amount of clathrin at the plasma membrane, but rather an ROS-dependent mechanism. Nevertheless, treatment of cells with low concentrations of exogenous hydrogen peroxide, corresponding to the amount produced in response to cryptogein (0.01–0.1 mM), did not trigger a significant FM4-64 internalization (data not shown). This rules out a nonspecific, stress-related effect on the observed endocytotic process.

We conclude that ROS production specifically produced via NtrbohD in response to the cryptogein is necessary for clathrin endocytosis to be triggered during early elicitation.

DISCUSSION

Endocytosis as an Early Signaling Event Elicited by Cryptogein

The membrane-selective fluorescent FM4-64 dye is a reliable marker to analyze the global endocytosis phenomenon and to visualize endosomes in plant cells (Bolte et al., 2004; Ueda et al., 2004). Real-time monitoring of FM4-64 internalization indicates that the rate of global endocytosis is higher in cryptogein-elicited cells at least in the first 15 min after treatment. In a recent study, similar stimulation in FM1-43 (a green-shift variant of FM4-64) dye uptake was reported in root cells of *Medicago truncatula* after *Sinorhizobium meliloti* inoculation, a symbiotic interaction that also induces a battery of trafficking genes (Peleg-Grossman et al., 2007). This induction is correlated with the fact that FM dye internalization is dependent on the vesicle transport machinery (Betz et al., 1996). We can thus propose that cryptogein triggers rapid membrane-trafficking events in tobacco cells.

The flat or invaginated pits, surrounded by dense particles forming a cage, which we have observed in tobacco cells using TEM, can be assumed to be different stages of CCP formation because it has already been described in plant cells (Low and Chandra, 1994; Robinson et al., 1998). Very recently, in plant cells, the nature of these cage-like molecules was confirmed with antibodies directed against plant clathrin heavy-chain peptides (Dhonukshe et al., 2007).

We evaluated the number of pits pinched off from the plasma membrane of 30 to 40 cells in ultrathin sections for each condition. In cryptogein-elicited cells, we observed a significant transitory CCP increase in the first 10 min, which may correspond to activation of the endocytosis machinery during this time lapse. Because we did consider the internalized CCVs, which may no longer be coated within the cytosol (Holstein, 2002), the results, corresponding to appearance of CCPs at the plasma membrane, are not directly comparable with FM4-64 experiments in which all fluorescent vesicles were counted. However, both indicate very early stimulation of endocytosis upon elicitor treatment. Moreover, these results can be related to the work of Fomina et al. (2003), who used FM1-43 dye to show accelerated endocytosis in phytohemagglutinin-activated lymphocyte T cells compared to resting cells and argued that the dye follows the CCV pathway within cells. Finally, very recently in Arabidopsis and tobacco BY-2 cells, genetic interference using the C-terminal clathrin heavy chain (so-called hub domain), which prevents clathrin cage formation, has been shown to inhibit FM4-64 uptake proving for a large part its clathrin dependence (Dhonukshe et al., 2007; Tahara et al., 2007).

Here, studies using microscopy and pharmacology are complementary and support the same conclusion: elicitation by cryptogein stimulates endocytosis and clathrin-coated endocytosis, in particular. The only other demonstration of an elicitor inducing an endocytotic process is the recent report in Arabidopsis of the internalization of the flagellin receptor-like kinase receptor after binding of the ligand, but the type of endocytosis was not characterized (Robatzek et al., 2006).

Thus, our results present evidence for induction of clathrin endocytosis by an elicitor of defense in plant cells, in addition to constitutive endocytosis.

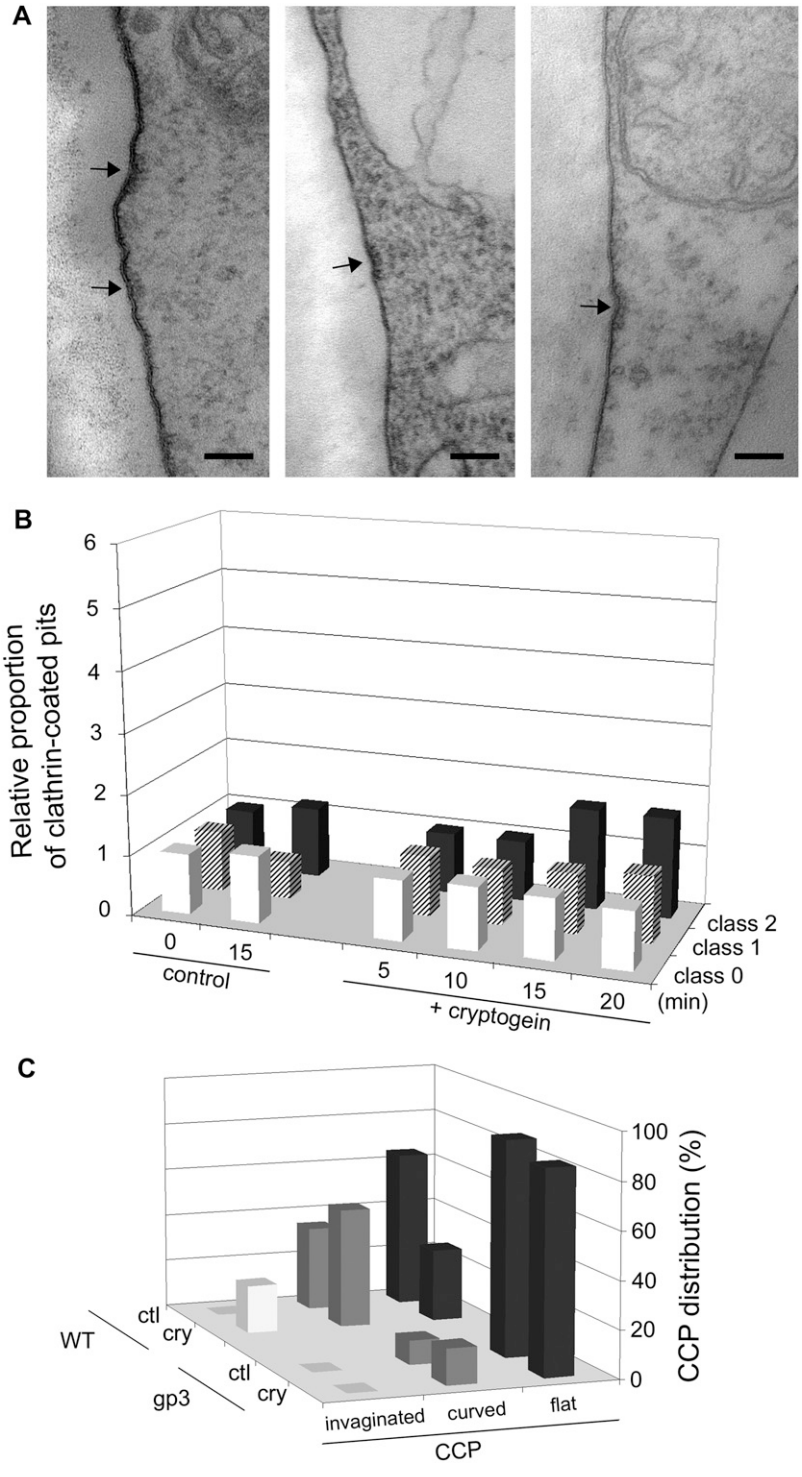

Figure 6. Cryptogein-stimulated endocytosis does not occur in cells inhibiting ROS production. The morphology of gp3 cells (antisense line of NADPH oxidase NtrbohD), which no longer produce ROS, was imaged by TEM. CCPs (arrows) were observed and quantified. A, Micrographs of three representative cell sections showing flat pits delimited at the intracellular face by a clathrin electron-dense coating (arrows). Bars = 100 nm. B, Relative increase of CCPs in gp3 cells in the absence or presence of 50 nM cryptogein; cell sections presenting no CCP (class 0), one CCP (class 1), or two or more CCP (class 2) within a 100-μm membrane perimeter (n = 20–30). C, Distribution of CCPs according to their shape in elicited (cry) or nonelicited (ctl) wild-type and gp3 cells after 15 min. Three classes of CCP were defined as a function of their diameter: flat (90–120 nm), curved (70–90 nm), and invaginated (40–70 nm). n = 20 to 30 cell sections.

ROS Production Is Correlated with Endocytosis

The use of LTP, a cryptogein antagonist that binds to the same high-affinity site at the plasma membrane, but triggers neither signaling events (Buhot et al., 2001) nor endocytosis (this study), emphasizes the role of signaling by cryptogein as the release mechanism for endocytosis. Interestingly, the transient wave of CCPs observed in the first 10 min after cryptogein addition exhibits the same kinetics as the typical transient production of ROS (Simon-Plas et al., 1997).

The oxidative burst is a typical early response of plant cells to elicitors and represents a characteristic feature of the HR, although its role in the associated signaling cascade remains to be clarified (Lamb and

Dixon, 1997; Torres and Dangl, 2005). ROS production induced in tobacco cells by cryptogein is due to a plasma membrane NADPH oxidase, NtrbohD (Simon-Plas et al., 2002). In this study, we show that transgenic cells inactivated for *NtrbohD* do not present cryptogein-stimulated clathrin endocytosis, although some other signaling events triggered by the elicitor, such as extracellular alkalinization, are identical to those observed in wild-type cells. These different observations suggest that the cryptogein-dependent oxidative burst is strongly correlated with cryptogein-mediated endocytosis events. A similar observation was made in Arabidopsis, where two chemicals that inhibit ROS production, triggered by the bacterial elicitor flagellin, were also inhibitors of flagellin receptor FLS2 endocytosis (Serrano et al., 2007). Interestingly, the observation of mainly flattened pits at the plasma membrane of gp3 cells may be related to the reduction of pinching off of FLS2-GFP containing buds in the presence of these two chemical compounds (Serrano et al., 2007).

Because the amount of clathrin proteins at the plasma membrane does not vary in wild-type or gp3 cells following cryptogein treatment, the regulatory effect of ROS on elicitor-induced endocytosis is likely to affect particular stages of CCV formation. The very short delay between the addition of cryptogein, ROS production, and the endocytotic processes does not suggest ROS-mediated activation of the transcriptional machinery.

Pharmacological Interference Supports a Role for RME in Cryptogein Signaling

CCPs constitute a major membrane entry point involved in RME in animal cells. It is well known that the cytosolic tails of receptors at the plasma membrane recruit clathrin to mediate the curvature of the membrane that will lead to its invagination. This mechanism, which takes place through an internalization motif (e.g. YXXθ) that can interact with the μ2-adaptin subunit of the clathrin-associated adaptor complexes AP2, is also expected to be clathrin-mediated endocytosis or RME in plants (Holstein, 2002). This has been indirectly established for the tomato (*Lycopersicon esculentum*) LeEiX2 receptor of the fungal ethylene-inducing xylanase elicitor, which contains a Tyr-based motif functioning as an endocytotic signal (Ron and Avni, 2004). Moreover, some receptor-like kinases are localized in an FM4-64 positive compartment (Gifford et al., 2005), sometimes complexed with their ligand (Shah et al., 2002; Russinova et al., 2004), although these receptors undergo constitutive internalization. The cryptogein receptor has not been identified yet, but preliminary observations of colloidal gold-labeled cryptogein inside BY-2 cells 5 min after elicitor treatment suggest that the cryptogein receptor follows a similar route (J. Lherminier, unpublished data).

In mammalian cells, Banbury et al. (2003) presented the conformational specificity of diverse members of the tyrphostin family to inhibit Tf-R endocytosis. Some of these tyrphostins, such as tyrphostin A23, block the internalization of the receptor, whereas inactive tyrphostin (e.g. tyrphostin A51) has no effect on this process. The authors used for each tyrphostin a concentration 10 times higher than their specific IC_{50} (50% inhibition of initial activity) calculated for the EGFR kinase activity (Gazit et al., 1989). In plant cells, tyrphostins A23 and A51 were used at the concentration of 350 μM to inhibit human Tf-R uptake in Arabidopsis protoplasts (Ortiz-Zapater et al., 2006). These two compounds were tested at a lower concentration (30 μM) for their effect on the uptake of several membrane proteins, but the authors underlined that tyrphostins may also affect other processes than the one studied (Dhonukshe et al., 2007).

In the context of plant defense, the use of such pharmacological components may be tricky because Tyr kinase inhibition could disturb cryptogein signaling because protein phosphorylation is involved in the initial step of cryptogein signal transduction (Viard et al., 1994). In the plant defense model Arabidopsis/flagellin (FLS2), substitution of a conserved potential phosphorylation site in the FLS2 receptor kinase or the general kinase inhibitor (K252a) impairs both endocytosis of the receptor as well as all tested FLS2-dependent immune responses (Robatzek et al., 2006).

In this study on tobacco cells, numbers of FM4-64-labeled vesicles and CCP both showed that cryptogein-stimulated endocytosis is differentially affected by a lower concentration (5 μM) of the two compounds. Indeed, tyrphostin A51 does not block elicitor-stimulated endocytosis, whereas tyrphostin A23 has a strong effect on this event. The inactivity of tyrphostin A51 argues against a mechanism involving Tyr kinase activity because tyrphostin A23 and tyrphostin A51 have an IC_{50} (on the human EGFR kinase activity) of 35 and 0.8 μM, respectively.

Concerning the effect of tyrphostins on the signaling events triggered by cryptogein, the extracellular alkalinization induced by the elicitor is not affected by the tested compounds, whereas ROS production is partially inhibited. This reinforces the hypothesis of a specific signaling pathway in which both ROS and endocytosis could be associated. However, the fact that the tyrphostins A51 and A23 have quite different effects on the endocytotic process, but not on ROS production, rules out an indirect effect on endocytosis through an inhibition of ROS production by tyrphostin A23.

These results show an inhibition of clathrin-mediated endocytosis by an RME inhibitor in a plant defense signaling context. The fact that tyrphostin A23 alone does not inhibit FM4-64 uptake of untreated cells (this study; Ortiz-Zapater et al., 2006; Dhonukshe et al., 2007), indicates that constitutive endocytotic traffic can continue in the presence of this inhibitor. This suggests that, although constitutive and cryptogein-induced endocytosis appears to be mediated by morphologically identical CCPs at the plasma membrane, the regulatory mechanisms involved could be different.

CONCLUSION

This study provides evidence for the involvement of CCPs/CCVs in the regulation of ligand-mediated endocytosis in plants. Increasing CCP formation in the first minutes following elicitation by cryptogein suggests that the endocytotic vesicles might assemble rapidly from predesignated plasma membrane domains that provide a platform for rapid and multiple production of vesicles. Recent papers propose that plant cell endocytosis, as in animal cells, is not only a mechanism for receptor down-regulation but also a prerequisite for signaling (Geldner et al., 2007; Robatzek, 2007). Because endocytosis and ROS production appear to be connected, the next challenging question is how ROS may affect the mechanism of endocytosis. Moreover, it will be interesting to localize endocytosis in the transduction pathway triggered by cryptogein.

MATERIALS AND METHODS

Material

Tobacco (*Nicotiana tabacum*) BY-2 cells and cells lacking *NtrbohD* expression (gp3 cells; Simon-Plas et al., 2002) were maintained under continuous light (200 μE m^{-2} s^{-1}) at 25°C on a rotary shaker (140 rpm). The suspensions were subcultured every 7 d at 1:20 mL dilution in Murashige and Skoog (1962) medium supplemented with 0.3 g L^{-1} Suc, 200 mg L^{-1} KH_2PO_4, 100 mg L^{-1} inositol, 2 g L^{-1} MES, 1 mg L^{-1} thiamine, and 0.2 mg L^{-1} 2,4-D. All experiments were performed with 7-d-old BY-2 cells harvested, filtered, and resuspended (1 g fresh weight for 10 mL) in I_2 buffer, a 2 mM MES buffer, pH 5.8, containing 175 mM mannitol, 0.5 mM $CaCl_2$, 0.5 mM K_2SO_4, for a 3-h equilibration period on a rotary shaker (140 rpm).

Fluorescent Probes and Chemicals

The fluorescent styryl membrane probe FM4-64 (Molecular Probes) was kept as a 17 mM stock solution in sterile water at 20°C (Bolte et al., 2004). This probe was used at the final concentration of 4.25 μM. Cryptogein was purified according to the method of Ricci et al. (1989), prepared in distilled water, and used at the final concentration of 50 nM. Tyrphostins A23 and A51 (Sigma-Aldrich) were stored in DMSO as 1,000-fold stock solutions and used at a final concentration of 5 μM. Wheat (*Triticum aestivum*) LTP1 was purified from wheat seeds as previously described (Charvolin et al., 1999), prepared in water, and used at the final concentration of 500 nM.

Live Microscopy of FM4-64 Internalization into Cells

To visualize endocytosis, the fluorescent styryl membrane probe FM4-64 was added to a 1-mL cell suspension in I_2 buffer, kept under shaking in the dark. After 5 min at room temperature (25°C), samples were taken before (time 0) and at different times (5–20 min) after addition of 500 nM LTP1 or 50 nM cryptogein and/or chemicals (0.1% DMSO or 5 μM tyrphostin solution in DMSO). Cell suspensions were mounted under a cover glass for microscopy and FM4-64 labeling was examined using a confocal microscope (TCS 4D; SP2 Leica Microsystems) equipped with an argon-krypton laser (488/515 BP-FITC). The laser was focused on cells through a 40× NA1 oil-immersion objective. FM4-64 emission was pass-filtered between 625 and 665 nm. Puncta were identified as endocytotic vesicles. Fluorescence measurements were performed with Image J software (http://rsb.info.nih.gov/ij/index.html).

TEM

Cell suspensions in I_2 buffer were sampled 5, 10, 15, and 20 min after elicitation with 50 nM cryptogein. Untreated cells were similarly sampled. When using tyrphostins A23 or A51 (5 μM in DMSO), sampling was performed under the same conditions, including controls with cryptogein treatment in the presence of DMSO without inhibitors. For each experiment, two independent assays were performed. Suspension cells were fixed in 100 mM sodium phosphate buffer (pH 7.2) containing 3% (v/v) glutaraldehyde and 2% (w/v) paraformaldehyde for 20 h at 4°C. After fixation, cells were washed several times in the same buffer for 30 min. Cells were then pelleted by low-speed centrifugation (1 min, 3,000 rpm) and embedded in 2.5% (w/v) agarose. Agarose blocks containing cells were then treated with 1% (w/v) osmium tetroxide in 100 mM sodium phosphate buffer for 1 h at 4°C and postfixed with 1% tannic acid in the same buffer for 30 min at room temperature in the dark. Cells were then dehydrated through a graded ethanol series and propylene oxide, and embedded in Epon (Spi-Chem) according to the standard procedure for conventional TEM (Luft, 1961). Ultrathin sections (80 nm) were cut on a Reichert Ultracut E ultramicrotome (Leica). They were collected on grids and counterstained with 3% (w/v) uranyl acetate in ethanol and lead citrate for conventional TEM. Sections were examined with a Hitachi H7500 transmission electron microscope (Hitachi Scientific Instruments Co.) operating at 80 kV and equipped with an AMT camera driven by AMT software (AMT). For each series, three embedded blocks were sectioned and for each block, 10 cells exhibiting 100-μm plasma membrane in the plane of the section were examined. For each sectioned cell, CCPs were quantified. Results were expressed in percentage of cells exhibiting 0, 1, or 2 and more CCP per 100 μm of plasma membrane.

AOS Production and Extracellular pH Modification

Cells were harvested 7 d after subculture, filtered, resuspended (1 g for 10 mL) in a 2 mM MES buffer, pH 5.90, containing 175 mM mannitol, 0.5 mM $CaCl_2$, and 0.5 mM K_2SO_4. After a 3-h equilibration period on a rotary shaker (150 rpm) at 25°C, cells were treated with cryptogein and/or chemicals as indicated in the legend of the Figure 5. The production of hydrogen peroxide was measured by chemiluminescence using luminol and a luminometer (BCL book; Berthold). Every 5 min, a 250-μL aliquot of the cell suspension was added to 50 μL of 0.3 mM luminol and 300 μL of the assay buffer (175 mM mannitol, 0.5 mM $CaCl_2$, 0.5 mM K_2SO_4, and 50 mM MES, pH 6.5). Extracellular pH modifications were monitored using a Radiometer pH meter.

ACKNOWLEDGMENTS

We are grateful to Francis Marty for helpful discussion. We thank Michel Ponchet (INRA, Sophia Antipolis) for providing purified cryptogein and Bénédicte Bakan (INRA, Nantes) for providing LTP1 from wheat. We also thank Nelly Debrosse and Mathieu Hanemian for their technical help, and Vivienne Gianinazzi-Pearson for critically reading the manuscript.

Received October 25, 2007; accepted December 21, 2007; published January 9, 2008.

LITERATURE CITED

Banbury DN, Oakley JD, Sessions RB, Banting G (2003) Tyrphostin A23 inhibits internalization of the transferrin receptor by perturbing the interaction between tyrosine motifs and the medium chain subunit of the AP-2 adaptor complex. J Biol Chem **278:** 12022–12028

Beguinot L, Lyall RM, Willingham MC, Pastan I (1984) Down-regulation of the epidermal growth factor receptor in KB cells is due to receptor internalization and subsequent degradation in lysosomes. Proc Natl Acad Sci USA **81:** 2384–2388

Betz WJ, Mao F, Bewick GS (1992) Activity-dependent fluorescent staining and destaining of living vertebrate motor nerve terminals. J Neurosci **12:** 363–375

Betz WJ, Mao F, Smith CB (1996) Imaging exocytosis and endocytosis. Curr Opin Neurobiol **6:** 365–371

Blein JP, Coutos-Thévenot P, Marion D, Ponchet M (2002) From elicitins to lipid-transfer proteins: a new insight in cell signalling involved in plant defence mechanisms. Trends Plant Sci **7:** 293–296

Blein JP, Milat ML, Ricci P (1991) Responses of cultured tobacco cells to cryptogein, a proteinaceous elicitor from *Phytophthora cryptogea*. Possible plasmalemma involvement. Plant Physiol **95:** 486–491

Bolte S, Talbott C, Boutte Y, Catrice O, Read ND, Satiat-Jeunemaître B (2004) FM-dyes as experimental probes for dissecting vesicle trafficking in living cells. J Microsc **214:** 159–173

Bonifacino JS, Traub LM (2003) Signals for sorting of transmembrane proteins to endosomes and lysosomes. Annu Rev Biochem **72:** 395–447

Brodsky FM (1988) Living with clathrin: its role in intracellular membrane traffic. Science **242:** 1396–1402

Buhot N, Douliez JP, Jacquemard A, Marion D, Trand V, Maume BF, Milat ML, Ponchet M, Mikès V, Kader JC, et al (2001) A lipid transfer protein binds to a receptor involved in the control of plant defence responses. FEBS Lett **509:** 27–30

Charvolin D, Douliez JP, Marion D, Cohen-Addad C, Pebay-Peyroula E (1999) The crystal structure of a wheat nonspecific lipid transfer protein (ns-LTP1) complexed with two molecules of phospholipid at 2.1 A resolution. Eur J Biochem **264:** 562–568

Crump CM, Williams JL, Stephens DJ, Banting G (1998) Inhibition of the interaction between tyrosine-based motifs and the medium chain subunit of the AP-2 adaptor complex by specific tyrphostins. J Biol Chem **273:** 28073–28077

Dhonukshe P, Aniento F, Hwang I, Robinson DG, Mravec J, Stierhof YD, Friml J (2007) Clathrin-mediated constitutive endocytosis of PIN auxin efflux carriers in Arabidopsis. Curr Biol **17:** 520–527

Dhonukshe P, Baluska F, Schlicht M, Hlavacka A, Samaj J, Friml J, Gadella TWJJ (2006) Endocytosis of cell surface material mediates cell plate formation during plant cytokinesis. Dev Cell **10:** 137–150

Fomina AF, Deerinck TJ, Ellisman MH, Cahalana MD (2003) Regulation of membrane trafficking and subcellular organization of endocytic compartments revealed with FM1-43 in resting and activated human T cells. Exp Cell Res **291:** 150–166

Garcia-Brugger A, Lamotte O, Vandelle E, Bourque S, Lecourieux D, Poinssot B, Wendehenne D, Pugin A (2006) Early signaling events induced by elicitors of plant defenses. Mol Plant Microbe Interact **19:** 711–724

Gazit A, Yaish P, Gilon C, Levitzki A (1989) Tyrphostins I: synthesis and biological activity of protein tyrosine kinase inhibitors. J Med Chem **32:** 2344–2352

Geldner N, Hyman DL, Wang X, Schumacher K, Chory C (2007) Endosomal signaling of plant steroid receptor kinase BRI1. Genes Dev **21:** 1598–1602

Gifford ML, Robertson FC, Soares DC, Ingram GC (2005) ARABIDOPSIS CRINKLY4 function, internalization, and turnover are dependent on the extracellular crinkly repeat domain. Plant Cell **17:** 1154–1166

González-Gaitán M (2003) Signal dispersal and transduction through the endocytic pathway. Nat Rev Mol Cell Biol **4:** 213–224

Holstein SE (2002) Clathrin and plant endocytosis. Traffic **3:** 614–620

Horn MA, Heinstein PF, Low PS (1989) Receptor-mediated endocytosis in plant cells. Plant Cell **1:** 1003–1009

Kwaaitaal MA, de Vries SC, Russinova E (2005) *Arabidopsis thaliana* Somatic Embryogenesis Receptor Kinase 1 protein is present in sporophytic and gametophytic cells and undergoes endocytosis. Protoplasma **226:** 55–65

Lamb C, Dixon RA (1997) The oxidative burst in plant disease resistance. Annu Rev Plant Physiol Plant Mol Biol **48:** 251–275

Low PS, Chandra S (1994) Endocytosis in plants. Annu Rev Plant Physiol Plant Mol Biol **45:** 609–631

Luft JH (1961) Improvements in epoxy resin embedding methods. J Biophys Biochem Cytol **9:** 409–414

Murashige T, Skoog F (1962) A revised medium for rapid growth and bioassays with tobacco tissue cultures. Physiol Plant **15:** 473–497

Murphy AS, Bandyopadhyay A, Holstein SE, Peer WA (2005) Endocytotic cycling of PM proteins. Annu Rev Plant Biol **56:** 221–251

Ortiz-Zapater E, Soriano-Ortega E, Marcote MJ, Ortiz-Masia D, Aniento F (2006) Trafficking of the human transferrin receptor in plant cells: effects of tyrphostin A23 and brefeldin A. Plant J **48:** 757–770

Parton RG, Richards AA (2003) Lipid rafts and caveolae as portals for endocytosis: new insights and common mechanisms. Traffic **4:** 724–738

Pastan I, Willingham MC (1985) Endocytosis. Plenum Press, New York

Peleg-Grossman S, Volpin H, Levine A (2007) Root hair curling and Rhizobium infection in *Medicago truncatula* are mediated by phosphatidylinositide-regulated endocytosis and reactive oxygen species. J Exp Bot **58:** 1637–1649

Pugin A, Frachisse JM, Tavernier E, Bligny R, Gout E, Douce R, Guern J (1997) Early events induced by the elicitor cryptogein in tobacco cells: involvement of a plasma membrane NADPH oxidase and activation of glycolysis and the pentose phosphate pathway. Plant Cell **9:** 2077–2091

Ricci P, Bonnet P, Huet JC, Sallantin M, Beauvaiscante F, Bruneteau M, Billard V, Michel G, Pernollet JC (1989) Structure and activity of proteins from pathogenic fungi *Phytophthora* eliciting necrosis and acquired resistance in tobacco. Eur J Biochem **183:** 555–563

Robatzek S (2007) Vesicle trafficking in plant immune responses. Cell Microbiol **9:** 1–8

Robatzek S, Chinchilla D, Thomas Boller T (2006) Ligand-induced endocytosis of the pattern recognition receptor FLS2 in Arabidopsis. Genes Dev **20:** 537–542

Robinson DG, Hinz G, Holstein S (1998) The molecular characterization of transport vesicles. Plant Mol Biol **38:** 49–76

Ron M, Avni A (2004) The receptor for the fungal elicitor ethylene-inducing xylanase is a member of a resistance-like gene family in tomato. Plant Cell **16:** 1604–1615

Russinova E, Borst JW, Kwaaitaal M, Cano-Delgado A, Yin Y, Chory J, de Vries SC (2004) Heterodimerization and endocytosis of Arabidopsis brassinosteroid receptors BRI1 and AtSERK3 (BAK1). Plant Cell **16:** 3216–3229

Serrano M, Robatzek S, Torres M, Kombrink E, Somssich IE, Robinson M, Schulze-Lefert P (2007) Chemical interference of PAMP-triggered immune responses in Arabidopsis reveals a potential role for FAS II complex-derived lipid signals. J Biol Chem **282:** 6803–6811

Shah K, Russinova E, Gadella TWJ, Willemse J, de Vries SC (2002) The Arabidopsis kinase-associated protein phosphatase controls internalization of the Somatic Embryogenesis Receptor Kinase 1. Genes Dev **16:** 1707–1720

Simon-Plas F, Elmayan T, Blein JP (2002) The plasma membrane oxidase NtrbohD is responsible for AOS production in elicited tobacco cells. Plant J **31:** 137–147

Simon-Plas F, Rustérucci C, Milat ML, Humbert C, Montillet JL, Blein JP (1997) Active oxygen species production in tobacco cells elicited by cryptogein. Plant Cell Environ **20:** 1573–1579

Tahara H, Yokota E, Igarashi H, Orii H, Yao M, Sonobe S, Hashimoto T, Hussey PJ, Shimmen T (2007) Clathrin is involved in organization of mitotic spindle and phragmoplast as well as in endocytosis in tobacco cell cultures. Protoplasma **230:** 1–11

Tavernier E, Wendehenne D, Blein JP, Pugin A (1995) Involvement of free calcium in action of cryptogein, a proteinaceous elicitor of hypersensitive reaction in tobacco cells. Plant Physiol **109:** 1025–1031

Taylor DR, Watt NT, Perera WSS, Hooper NM (2005) Assigning functions to distinct regions of the N-terminus of the prion protein that are involved in its copper-stimulated, clathrin-dependent endocytosis. J Cell Sci **118:** 5141–5153

Torres MA, Dangl JL (2005) Functions of the respiratory burst oxidase in biotic interactions, abiotic stress and development. Curr Opin Plant Biol **8:** 397–403

Ueda T, Uemura T, Sato MH, Nakano A (2004) Functional differentiation of endosomes in Arabidopsis cells. Plant J **40:** 783–789

Viard MP, Martin F, Pugin A, Ricci P, Blein JP (1994) Protein phosphorylation is induced in tobacco cells by the elicitor cryptogein. Plant Physiol **104:** 1245–1249

Watts C (1985) Rapid endocytosis of the transferrin receptor in the absence of bound transferrin. J Cell Biol **100:** 633–637

Wendehenne D, Binet MN, Blein JP, Ricci P, Pugin A (1995) Evidence for specific, high-affinity binding sites for a proteinaceous elicitor in tobacco plasma membrane. FEBS Lett **374:** 203–207

Wendehenne D, Lamotte O, Frachisse JM, Barbier-Brygoo H, Pugin A (2002) Nitrate efflux is an essential component of the cryptogein signaling pathway leading to defense responses and hypersensitive cell death in tobacco. Plant Cell **14:** 1937–1951